Perilipin 5 and liver fatty acid binding protein function to restore quiescence in mouse hepatic stellate cells[S]

Jianguo Lin,*,† Shizhong Zheng,§ Alan D. Attie, Mark P. Keller,** David A. Bernlohr,†† William S. Blaner,§§ Elizabeth P. Newberry,*** Nicholas O. Davidson,[1],*** and Anping Chen[1],***

Department of Pathology,* School of Medicine, Saint Louis University, St. Louis, MO; Department of Neurology,† Guangdong Second Provincial General Hospital, Guangzhou, China; Department of Pharmacology,§ School of Pharmacy, Nanjing University of Chinese Medicine, Nanjing, China; Department of Biochemistry, Molecular Biology and Biophysics,** University of Wisconsin, Madison, WI, 53706; Department of Biochemistry, Molecular Biology and Biophysics,†† University of Minnesota, Minneapolis, MN 55455; Department of Medicine,§§ Columbia University, New York, NY 10032; Gastroenterology Division,*** Washington University School of Medicine, St. Louis, MO 63110

Abstract **Hepatic stellate cell (HSC) activation occurs along with decreased Perilipin5 (Plin5) and liver fatty acid-binding protein (L-Fabp) expression and coincident lipid droplet (LD) depletion. Conversely, the activated phenotype is reversible in WT HSCs upon forced expression of Plin5. Here, we asked if L-Fabp expression is required for Plin5-mediated rescue of the quiescent phenotype. Lentiviral Plin5 transduction of passaged *L-Fabp*$^{-/-}$ HSCs failed to reverse activation markers or restore lipogenic gene expression and LD formation. However, adenoviral L-Fabp infection of lentiviral Plin5 transduced *L-Fabp*$^{-/-}$ HSCs restored both the quiescent phenotype and LD formation, an effect also mediated by adenoviral intestine-Fabp or adipocyte-Fabp. Expression of exogenous Plin5 in activated WT HSCs induced a transcriptional program of lipogenic gene expression including endogenous L-Fabp, but none of the other FABPs. We further demonstrated that selective, small molecule inhibition of endogenous L-Fabp also eliminated the ability of exogenous Plin5 to rescue LD formation and reverse activation of WT HSCs. This functional coordination of L-Fabp with Plin5 was 5′-AMP-activated protein kinase (AMPK)-dependent and was eliminated by AMPK inhibition.** **Taken together, our results indicate that L-Fabp is required for Plin5 to activate a transcriptional program that restores LD formation and reverses HSC activation.**—Lin, J., S. Zheng, A. D. Attie, M. P. Keller, D. A. Bernlohr, W. S. Blaner, E. P. Newberry, N. O. Davidson, and A. Chen. **Perilipin 5 and liver fatty acid binding protein function to restore quiescence in mouse hepatic stellate cells.** ***J. Lipid Res.*** **2018.** 59: **416–428.**

Supplementary key words lipid droplets • perilipins • fatty acid-binding proteins • lipid metabolism • stellate cell activation

Nonalcoholic fatty liver disease encompasses a spectrum of pathology ranging from simple steatosis to nonalcoholic steatohepatitis (NASH) and cirrhosis, but the mechanisms and mediators that regulate necroinflammation and disease progression are still poorly understood (1–3). NASH-associated hepatic fibrosis is currently the target of significant scientific and clinical interest, in particular, the mechanisms regulating activation of hepatic stellate cells (HSCs), which are the major fibrogenic effectors (1–3). Quiescent HSCs contain abundant complex lipids that are localized within lipid droplets (LDs) (1–3). Upon HSC activation and the induction of fibrogenesis, HSCs undergo loss of LDs along with enhanced proliferation, de novo expression of α-smooth muscle actin (α-SMA), and overproduction of extracellular matrix, including αI(I) collagen.

Among the most abundant proteins on LDs are members of the perilipin (Plin) family of lipid droplet proteins, some of which (e.g., Plin2) play important roles in the regulation of lipid metabolism in a variety of tissues including liver (4–7). Our previous observations demonstrated that

This work was supported by the Doisy Research Fund and a Research Award from the Saint Louis University Liver Center (to A. C.). N.O.D. was supported by grants from the National Institutes of Health (HL-38180, DK-112378, DK-56260, DK-52574, Murine and Advanced Imaging Cores). This work was also supported by grants from the National Institutes of Health, the Wisconsin Alumni Research Foundation (WARF), and the University of Wisconsin Institute for Clinical and Translational Research (ICTR; to A.D.A. and M.P.K.) W.S.B. was supported by grants from the National Institutes of Health (RO1 DK-068437 and RO1 DK-101251). The content is solely the responsibility of the authors and does not necessarily represent the official views of the National Institutes of Health.

Manuscript received 3 May 2017 and in revised form 7 December 2017.

Published, JLR Papers in Press, January 9, 2018
DOI https://doi.org/10.1194/jlr.M077487

Abbreviations: abhd5, abhydrolase domain containing 5; ACC, acetyl coA carboxylase; AMPK, AMP-activated protein kinase; 1, 8 ANS, 8-anilinonaphthalene-1-sulfonic acid; ATGL, adipose triglyceride lipase; Ad-L-Fabp, adenoviral liver Fabp; Ad-I-Fabp, adenoviral intestine-Fabp; Ad-A-Fabp, adenoviral adipocyte-Fabp; α-SMA, α-smooth muscle actin; HSC, hepatic stellate cell; LD, lipid droplet; LOX-1, lectin-like oxidized LDL receptor-1; L-Fabp, liver fatty acid-binding protein; LRAT, lecithin-retinol acyltransferase; LV, lentiviral; LXR, liver X receptor; NSOP313, NSOP00313; NASH, nonalcoholic steatohepatitis; PKA, protein kinase A; Plin 5, perilipin 5; PPRE, peroxisome proliferator response element; TG, triglyceride; YFP, yellow fluorescent protein.

[1]To whom correspondence should be addressed.
e-mail: achen5@slu.edu (A.C.); nod@wustl.edu (N.O.D.).

[S] The online version of this article (available at http://www.jlr.org) contains a supplement.

activation of WT mouse HSCs was coupled to a dramatic reduction in expression of Plin5, both in vitro and in vivo (8). In addition, other work in *Plin5* knockout mice indicated that Plin5 prevented hepatic lipotoxicity, suggesting a broader role for this LD protein in the regulation of hepatic fibrogenesis (9). In keeping with this suggestion, we recently reported that exogenous Plin5 significantly increased intracellular lipid content and restored LDs in HSCs from WT mice (8). In addition, the expression of exogenous Plin5 attenuated intracellular oxidative stress in WT HSCs (8). These actions collectively resulted in attenuated HSC activation (8) and support the concept that preserving lipid content by modulating turnover of HSC LDs may promote a quiescent state (10, 11) and could be a functional strategy for inhibiting fibrogenesis (10, 11).

Other players involved in HSC lipid metabolism include members of the fatty acid-binding protein (FABP) family of lipid-binding proteins, which are involved in the uptake, transport, and metabolism of FAs, retinoids, and other lipid ligands (12). Among these FABPs, liver Fabp (L-Fabp, Fabp1) is abundantly expressed in both hepatocytes and enterocytes and plays a key role in high-fat diet-induced hepatic steatosis (13–17) and also in the development and progression of diet-induced NASH in vivo (18). L-Fabp is also abundantly expressed in quiescent HSCs, and our previous work demonstrated that activation of WT HSCs is coupled to decreased L-Fabp expression, temporally related to LD depletion, and reversed upon adenoviral-mediated L-Fabp rescue (18).

Here, we sought to expand understanding of the pathways that regulate HSC activation and LD turnover in relation to mechanisms of lipid-mediated liver injury. Our specific questions centered on the role of L-Fabp expression as a requisite component of Plin5-mediated rescue of HSC quiescence, including LD formation and reversal of the activated phenotype.

MATERIALS AND METHODS

Animal studies

The animal protocols for the use of mice in this study were approved by the Institutional Animal Care and Use Committees of Saint Louis University and Washington University in St. Louis and followed guidelines issued by the National Institutes of Health. Congenic *L-Fabp* knockout mice (*L-Fabp*$^{-/-}$) were generated and maintained as described previously (18). WT male and female C57BL/6J mice were purchased from Jackson Laboratory, Bar Harbor, MA, and were housed in a temperature-controlled animal facility (23°C) with a 12:12 h light-dark cycle and allowed free access to regular chow and water. Male and female WT and *L-Fabp*$^{-/-}$ mice were maintained on a standard rodent chow diet (PicoLab Rodent Diet 20) and mice of comparable ages (12–16 weeks) were used for isolation of HSCs for experiments.

Isolation and culture of HSCs

HSCs were isolated by pronase-collagenase perfusion in situ before density gradient centrifugation, as previously described (19). Freshly isolated HSCs were cultured in DMEM supplemented with 20% FBS. Cells were passaged in DMEM with 10% FBS. Unless otherwise indicated, semi-confluent HSCs with four to nine passages were used in all experiments. In some experiments, lentivirus transduced HSCs were treated with L-Fabp inhibitors (supplemental Fig. S1), at the indicated doses for 24 h. All FABP inhibitors were synthesized by a commercial vendor on a contract basis (Nanosyn, Santa Clara, CA). Compound purity was determined by LC-MS, and was >98% for all compounds. The design of these inhibitors was based on structural similarity to 8-anilinonaphthalene-1-sulfonic acid (1, 8 ANS), which contains both a sulfonic acid and an amine group and competes for binding within the ligand binding pocket of hydrophobic ligand binding proteins as determined using a displacement assay as previously described (20). Purified recombinant FABP from liver, intestine, epithelium, heart, and adipose were used to evaluate compound selectivity experimentally. 1,8-ANS fluorescence (480 nm emission; 397 nm excitation) was determined in response to 6 μM purified FABP protein, 500 nM 1,8-ANS, and varying amounts of one of the test compounds in a final volume of 50 μl. A ten-point compound concentration series ranging from 0.7 – 100 μM was used to determine an IC_{50} for each compound to displace 1,8-ANS from the ligand-binding pocket of each FABP isoform. Oleic acid was used as a positive control, and yielded an apparent IC_{50} of ~7 μM. Compounds NSOP313 and NSOP373 were the most selective for liver FABP, with IC_{50} values of 3.7 μM and 7.2 μM, respectively; for all other FABP isoforms, these compounds demonstrated IC_{50} values >100 μM. Compounds NSOP318 and NSOP364 were the most potent for liver FABP, with IC_{50} values of 1.5 μM and 1.8 μM, but substantial binding to the adipose and epithelial FABP isoforms was observed. NSOP325 was the least potent compound for liver FABP (IC50 ~9 μM), and showed significant binding to all five FABP isoforms. Owing to the combination of high potency and selectivity toward liver FABP, NSOP313 was used for the studies reported. Where indicated, the AMPK inhibitor Compound C (Sigma, St Louis, MO) was added as indicated in the Fig. 6 legend at a dose of 20 μM (8).

RNA extraction and real-time PCR

Total RNA was extracted from cells by TRI-Reagent, following the protocol recommended by the manufacturer (Sigma). Total RNA was treated with DNase I before the synthesis of the first strand of cDNA. Real-time PCR was performed as previously described using SYBR Green Supermix (21). mRNA levels were expressed as fold change after normalization with GAPDH, as described by Schmittgen et al. (22). Threshold cycle (Ct) value used in this report for the housekeeping gene GAPDH was 18–20. Ct values for other target genes and corresponding controls were within a range of 25–30. Representative Ct values for Plin5 in quiescent and activated HSCs are reported in the figure legend for Fig. 1. Fold change values are presented as $2^{-\Delta\Delta Ct}$. Ct values higher than 35 were considered not detectable. The primers used in real-time PCR were previously described (8).

Recombinant expression constructs, antisera, and immunoblots

Construction of the recombinant lentiviral (LV)-Plin5-yellow fluorescent protein (YFP) and the control LV-YFP were as previously described (8). Recombinant adenoviral (Ad)-L-Fabp with expression of FLAG epitope-tagged L-Fabp, or recombinant adenoviral Ad-LacZ with expression of LacZ were previously described and used (18). Ad-I-Fabp was constructed using a mouse I-Fabp cDNA containing three copies of the FLAG epitope tag at the N terminus and cloned into the pVQ AdCMV shuttle plasmid for recombination, amplification, and purification (ViraQuest Labs). Ad-A-Fabp was generated as previously described (23). In brief, the expression construct was recombined into pADEasy in *Escherichia coli* BJ5183 cells and transfected (Lipofectamine, Invitrogen) into 293 cells (American Type Culture Collection, Manassas,

VA) to allow packaging and amplification. Large scale adenovirus preparations were obtained from 10 cm plates in which the media was collected, centrifuged at 20,000 *g* for 10 min to pellet the cellular debris, and the supernatant containing virus particles recovered and frozen in aliquots at −70°C. Antisera to FABPs and perilipins were previously described (16). Western blotting analyses were conducted as we previously described (8). Thirty micrograms of proteins per well were used in all immunoblots, except where indicated as in Fig. 1.

Knockdown of perilipin 2 by shRNA

The RNAi sequences targeting mouse Plin2 mRNA was selected using online RNAi design program from Thermo Fisher Scientific, Dharmacon RNAi Technologies (Lafayette, CO). Three shRNA constructs were generated and tested. The best inhibitory results were from the following Plin2 shRNA sequence: 5′-GGA CCA AGT CTG TGG TCA A-3′. The anti-sense sequence of the Plin2 shRNA was used as a negative control. Construction of shRNA expression cassettes and subsequent cloning in the lentiviral vector pFLRu were conducted as we previously described (24).

Plasmids, transient transfection, and luciferase activity assays

The luciferase reporter plasmid pPPRE-Luc contains three copies of peroxisome proliferator response elements (PPREs) from the acyl-CoA oxidase gene, as we previously described (25). The luciferase reporter plasmid LXR-Luc has three copies of liver X receptor (LXR) binding elements. It was a gift from Dr. Knut Steffensen (26). The plasmid TOPFlash is a Wnt/β-catenin signaling luciferase activity reporter. It was kindly provided by Dr. Randall Moon (27). Plasmid transfection and luciferase activity assays were undertaken as previously described (28).

In situ quantification of LDs and lipid assays

Oil Red O staining was undertaken on HSCs seeded on autoclaved cover slips in a 6-well plate and cultured in DMEM with 10% FBS with or without transduction and/or treatment, followed by fixation with 4% paraformaldehyde (30 min). LDs were stained as previously described (28). Numbers of LDs in Oil Red O-stained HSCs were quantified using the Nuance multispectral imaging system (Perkin-Elmer, MA), as we previously described (18). Cells of interest were digitized and circled individually within the image and the numbers of LDs per cell automatically calculated. Positive staining was adjusted by subtracting background control signals. The results were collected and expressed as a mean number of LDs per cell based on at least 10 cells. Intracellular FFAs and triglycerides (TG) were colorimetrically determined using kits from BioVision, Inc. (Mountain View, CA), following the manufacturer's protocol (29).

Fatty acid uptake and lipolysis assays

WT-passaged HSCs were transduced with or without LV-Plin5-YFP, or LV-YFP, or LV-Plin5-YFP plus Ad-L-Fabp. Cells were incubated in media containing 2μCi [3H]oleic acid (ART 0198, American Radiolabeled Chemicals, St. Louis, MO) and 250 μM oleic acid albumin (O-3008, Sigma-Aldrich) for 4 h at 37°C, washed, and extracted with chloroform-methanol as described (15). Radiolabeled lipids were separated by thin layer chromatography, and the position of 3H-lipids was determined by migration of unlabeled standards. Assays were performed in triplicate, and normalized to cellular protein content.

For lipolysis assays, cells (groups as described above) were collected in PBS and frozen. Cell pellets were homogenized in 0.25M sucrose, 1 mM EDTA, 1 mM DTT, with protease inhibitors and centrifuged at 1,000 *g* to remove insoluble material. Lipase activity was measured using 0.5 μCi [3H]Triolein (ART 0199, American Radiolabeled Chemicals) in the presence of 80 μM glyceryl trioleate (T-7140, Sigma-Aldrich) and 1% FA-free BSA for 1 h at 37°C. Assays were stopped by the addition of chloroform-methanol, extracted, and analyzed by thin layer chromatography as described above, and regions comigrating with unlabeled oleate were scraped and counted. Data were corrected for nonspecific hydrolysis and normalized to cellular protein.

Analysis of cellular retinol and retinyl esters

WT-passaged HSCs were transduced with or without LV-Plin5-YFP, or LV-YFP, or LV-Plin5-YFP plus Ad-L-Fabp. HSC concentrations of retinol and retinyl esters were determined by HPLC protocols described previously (30). Briefly, frozen HSC pellets were resuspended and homogenized in 1.0 ml of ice-cold PBS (10 mM sodium phosphate, pH 7.2, 150 mM sodium chloride) using a Polytron homogenizer (Brinkmann Instruments, Westbury, NY) set at half-maximal speed for 10 s. The HSC homogenate was then treated with an equal volume of absolute ethanol containing a known amount of retinyl acetate as an internal standard. The retinoids present in the homogenates were extracted into hexane. After one backwash against doubly distilled water, the hexane extract was evaporated to dryness under a gentle stream of nitrogen. Immediately upon reaching dryness, the retinoid-containing film was redissolved in 40 μL of benzene for injection onto the HPLC column. The extracted retinoids were separated on a 4.6 × 250 mm Ultrasphere C18 column (Beckmann, Fullerton, CA) preceded by a C18 guard column (Supelco, Bellefonte, PA) using 70% acetonitrile-15% methanol-15% methylene chloride as the running solvent flowing at 1.8 ml/min. Retinol and individual retinyl esters (retinyl palmitate, oleate, linoleate, and stearate) were detected at 325 nm and identified by comparing the retention times and spectral data of experimental compounds with those of authentic standards. Concentrations of retinol and retinyl esters in the HSCs were quantitated by comparing integrated peak areas of each retinoid against those of known amounts of purified standards. Loss during extraction was accounted for by adjusting for the recovery of internal standard added immediately after homogenization of the samples.

Statistical analyses

Differences between means were evaluated using an unpaired two-sided Student's *t*-test ($P < 0.05$ considered as significant). Where appropriate, comparisons of multiple treatment conditions with controls were analyzed by ANOVA with the Dunnett's test for post hoc analysis.

RESULTS

L-Fabp is critical for Plin5-mediated rescue of LD formation in HSCs

To determine the role of L-Fabp in Plin5-mediated rescue of LD formation, we examined cultured HSCs from WT and *L-Fabp*$^{-/-}$ mice, transduced with recombinant LV-Plin5-YFP or an empty lentiviral LV-YFP control. As shown in **Fig. 1A**, LV-Plin5-YFP (but not the empty vector control) restored the formation of LDs in activated WT HSCs, demonstrated by staining with Oil Red O. In contrast, LV-Plin5-YFP

failed to restore LD formation in HSCs from *L-Fabp*$^{-/-}$ mice (Fig. 1A).

We found that Plin5 was expressed in both freshly isolated WT and *L-Fabp*$^{-/-}$ HSCs (Fig. 1B, C), although the abundance of Plin5 mRNA was lower in *L-Fabp*$^{-/-}$ (Ct value ≈28.5) compared with WT HSCs (Ct value ≈28.1) (Day 1) (Fig. 1B). These findings led us to ask whether germline *L-Fabp* deletion impaired endogenous Plin5 expression in freshly isolated HSCs. However, Western blotting analyses of HSCs revealed comparable abundance of Plin5 at Day 0 in both genotypes (Fig. 1C). We further showed that Plin5 was reduced in HSCs of both genotypes after culture for 7 days (Day 7) (Fig. 1B and C), a time in culture that other studies have shown quiescent HSCs spontaneously become fully activated (31). Transduction of LV-Plin5-YFP resulted in a comparable increase in (exogenous) Plin5 expression in both passaged-WT and *L-Fabp*$^{-/-}$ HSCs (Fig. 1D). Considered together, these findings reveal expression of Plin5 protein in freshly isolated, quiescent HSCs in both genotypes, albeit at lower abundance than observed in passaged HSCs transduced with LV-Plin5 (compare Fig. 1C with Fig. 1D), particularly when taking into consideration that 40 μg total protein was loaded per well in Fig. 1C versus 20 μg in Fig. 1D. Nevertheless, the data established that Plin5

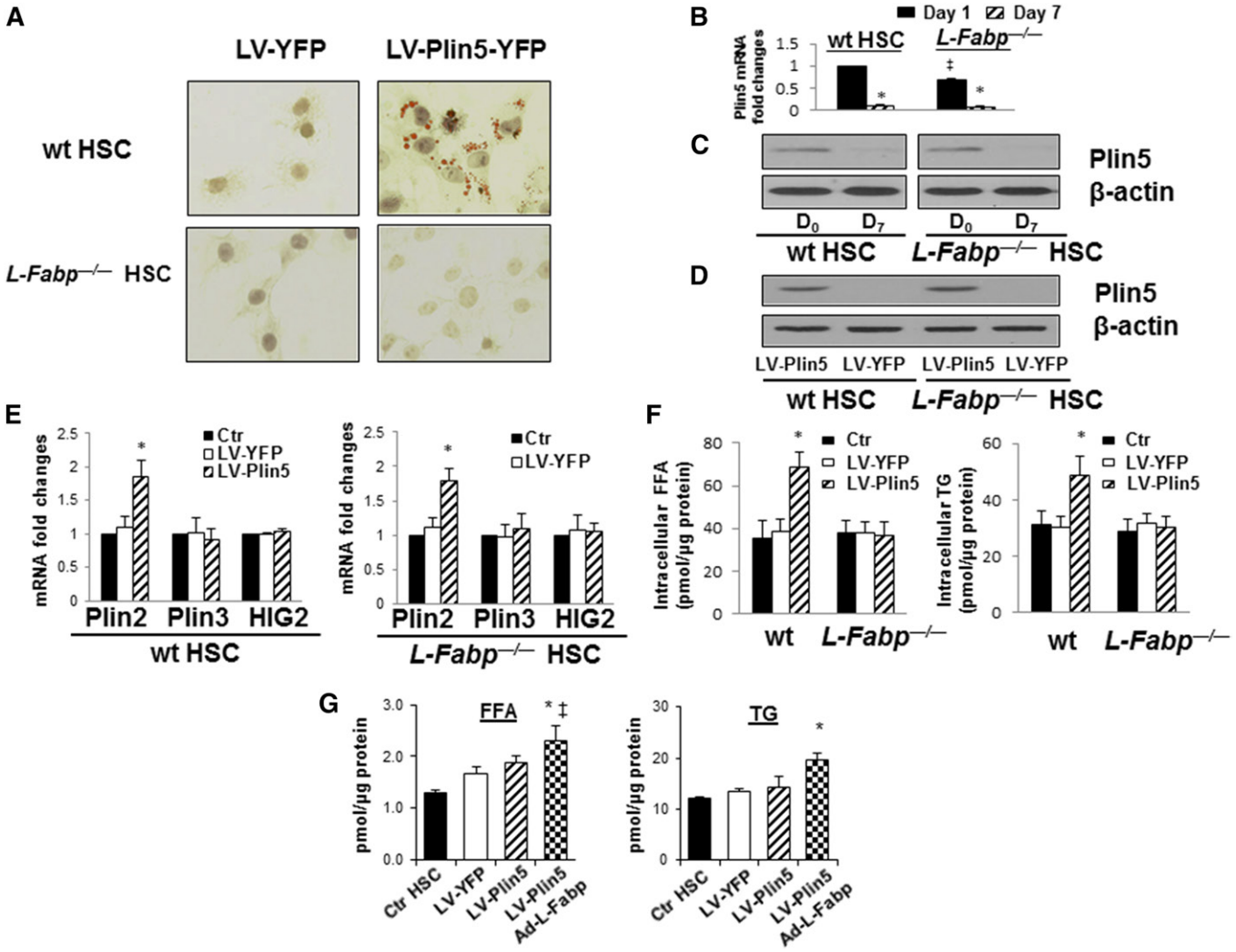

Fig. 1. L-Fabp is critical for Plin5-mediated rescue of LD formation in HSCs. Passaged HSCs from WT mice (wt HSC) and from L-Fabp germline knockout mice (*L-Fabp*$^{-/-}$HSC) were transduced with the recombinant lentiviral LV-Plin5-YFP or the empty lentiviral LV-YFP, respectively, as a vehicle mock control. Positive transductants were selected with puromycin at 5 μg/ml for 48 h. A: Oil Red O staining of cellular LDs. Representative views from three independent experiments are presented. B: Real-time PCR assays of Plin5 in freshly isolated WT HSCs or *L-Fabp*$^{-/-}$HSCs after culture for 1 day or 7 days (n = 3), $^{*}P < 0.05$ vs. corresponding HSCs at day 1, and $^{‡}P < 0.05$ vs wtHSCs at day 1 (Ct Plin5 in WT HSC ≈28.1; Ct Plin5 in *L-Fabp*$^{-/-}$HSC≈28.5; Ct GAPDH≈18). C: Western blotting analyses of Plin5 in freshly isolated WT HSCs or *L-Fabp*$^{-/-}$HSCs (D0) or after culture for 7 days (D7) (40 μg protein/well was loaded). β-actin was used as an invariant control for equal loading. D: Western blotting analyses of Plin5 in WT HSCs or *L-Fabp*$^{-/-}$HSCs, respectively, transduced with LV-YFP or LV-Plin5-YFP (20 μg protein/well was loaded). E: Real-time PCR analyses of expression of LD protein genes in wt HSCs and in *L-Fabp*$^{-/-}$HSCs (n = 3). $^{*}P < 0.05$ vs corresponding control (Ctr). F: Analyses of cellular FFA (n = 3), and cellular TG (n = 3) content following lentiviral transduction; $^{*}P < 0.05$ vs. corresponding nontransduced Ctr HSCs. G: Uptake of FA and incorporation into TG in wt HSCs following transduction with or without LV-YFP, LV-Plin5, or LV-Plin5 plus Ad-L-Fabp (n = 3); $^{*}P < 0.01$ vs. the CtrHSCs; $^{‡}P < 0.04$ vs. HSCs with LV-YFP.

expression from the lentiviral transduction experiments reflect a reasonable range of forced overexpression in relation to endogenous levels in freshly isolated HSCs.

Having established these baseline parameters, we next evaluated the role of Plin5 in regulating cellular lipid content in HSCs. We found that forced expression of exogenous Plin5 in both WT and *L-Fabp*$^{-/-}$ HSCs induced expression of Plin2 (Fig. 1E), but that the expression of other lipid droplet protein genes, including Plin3 and hypoxia-induced gene 2 (HIG2), were unaffected. We further examined the coordinated effects of Plin5 and L-Fabp in modulating cellular lipid content (Fig. 1F). As expected, LV-Plin5-YFP transduction increased intracellular FFA and TG content in WT but not *L-Fabp*$^{-/-}$ HSCs (Fig. 1F). In addition, we found that Plin5 and L-Fabp together promote uptake of radiolabed FA and TG formation in WT HSCs (Fig. 1G). These results collectively suggest that L-Fabp plays a permissive role, along with Plin5, in increasing cellular lipid content and restoring LD formation in WT HSCs. However, for reasons explored below, and despite comparable expression of exogenous Plin5 following lentiviral transduction, this response fails to occur in *L-Fabp*$^{-/-}$ HSCs.

L-Fabp is required for Plin5-mediated reversal of HSC activation and transcriptional induction of prolipogenic signaling pathways

To explore the underlying mechanisms by which Plin5 and L-Fabp function in promoting cellular lipid content, we asked whether exogenous Plin5 might stimulate prolipogenic and/or attenuate antilipogenic transduction pathways, in a manner dependent on L-Fabp. For this purpose, we examined LXR and PPARγ induction as models of prolipogenic induction (32–34) and also Wnt/β-catenin signaling which, via cross-talk with PPARγ, interferes with its functions and is considered antilipogenic (35, 36). We transduced WT or *L-Fabp*$^{-/-}$ HSCs with LV-Plin5-YFP or LV-YFP and after selection, transfected those cells with luciferase reporter plasmids LXR-Luc, PPRE-Luc, or TOP-Flash (see details in Methods). As shown in **Fig. 2A**, elevated luciferase activity was found in LXR-Luc and PPRE-Luc-transfected WT but not *L-Fabp*$^{-/-}$ HSCs transduced with Plin5. Conversely, we observed reduced luciferase activity in WT but not *L-Fabp*$^{-/-}$ HSCs transfected with TOPFlash-Luc and transduced with Plin5.

We further examined mRNA expression of acetyl coA carboxylase (ACC), FAS, and lectin-like oxidized LDL receptor-1 (LOX-1), which are surrogate downstream target genes of LXR (37), PPARγ (38) and Wnt/β-catenin signaling (39), respectively. We found that expression of exogenous Plin5 significantly increased mRNA abundance of ACC and FAS and reduced LOX-1 mRNA in WT but not *L-Fabp*$^{-/-}$ HSCs (Fig. 2B). Using the same experimental design, forced expression of Plin5 in WT, but not *L-Fabp*$^{-/-}$ HSCs, significantly inhibited mRNA abundance of α-SMA and αI(I) procollagen, two markers of fibrogenic activation (Fig. 2C). We also found that exogenous Plin5 significantly reduced mRNA abundance of pro-lipolytic genes patatin-like phospholipase-3, adipose triglyceride lipase (ATGL), and abhydrolase domain containing 5 (abhd5), in WT but not *L-Fabp*$^{-/-}$ HSCs (Fig. 2D). These changes were accompanied by induction of SREBP-1 and PPARγ mRNAs by 3- to 5-fold (Fig. 2D). As noted above, these effects of exogenous Plin5 on lipogenic gene expression were not observed in *L-Fabp*$^{-/-}$ HSCs (Fig. 2D). Taken together, these findings reinforce the conclusion that *L-Fabp* deletion significantly attenuates the ability of Plin5 to inhibit HSC activation and elevate cellular lipid content, likely through a network of transcriptional signaling pathways.

Introduction of L-Fabp into *L-Fabp*$^{-/-}$ HSCs rescues Plin5-mediated reversal of activation and prolipogenic activity

We introduced Ad L-Fabp (or LacZ control virus) into LV-Plin5-YFP or LV-YFP transduced *L-Fabp*$^{-/-}$ HSCs as detailed in Methods. Western blotting revealed (as expected) that endogenous L-Fabp in both passaged WT HSCs and *L-Fabp*$^{-/-}$ HSCs was not detectable, while Ad-L-Fabp transduction led to a comparable increase in L-Fabp expression in both genotypes (**Fig. 3A**). Real-time PCR analyses indicated that forced expression of L-Fabp induced expression of Plin5 in both passaged WT HSCs and *L-Fabp*$^{-/-}$ HSCs (Fig. 3B) as previously reported (18). As shown in Fig. 3C, upon rescue of L-Fabp expression in *L-Fabp*$^{-/-}$ HSCs, Plin5 transduction decreased expression of α-SMA and αI(I) procollagen mRNAs and also increased mRNA abundance of SREBP-1 and PPARγ (Fig. 3C). Forced L-Fabp expression also restored cellular FFA and TG content in Plin5 transduced *L-Fabp*$^{-/-}$ HSCs (Fig. 3D).

As noted above (Fig. 1A), Plin5 transduction into WT HSCs led to increased mRNA expression of Plin2. In view of prior studies demonstrating a role of Plin2 in LD formation in HSCs (40), we sought to clarify the role of Plin2 in the coordinated interactions of L-Fabp and Plin5 in LD formation. For this purpose, we cultured *L-Fabp*$^{-/-}$ HSCs with LV-YFP or LV-Plin5, with or without Ad-L-Fabp, in the presence of Plin2 shRNA. This knockdown strategy resulted in more than 80% Plin2 knockdown efficiency (Fig. 3E). We confirmed that exogenous Plin5 increased endogenous Plin2 protein expression in *L-Fabp*$^{-/-}$ HSCs, but Ad-L-Fabp rescue caused no further upregulation of Plin2 expression (Fig. 3E). Furthermore, Oil Red O staining revealed that shRNA inhibition of Plin2 had no effect on LD formation in *L-Fabp*$^{-/-}$ HSCs transduced with Plin5 and Ad L-Fabp (Fig. 3E). Finally, to examine the role of L-Fabp and Plin5 in coordinating transcriptional activation of lipogenic pathways, Ad-L-Fabp infected, Plin5 transduced *L-Fabp*$^{-/-}$ HSCs were transiently transfected with LXR-Luc, PPRE-Luc, or TOPFlash plasmids as above. Luciferase activity assays revealed that Ad-L-Fabp rescued Plin5-mediated transcriptional induction in *L-Fabp*$^{-/-}$ HSCs transfected with LXR-Luc or PPRE-Luc, and, conversely, reduced luciferase activities in *L-Fabp*$^{-/-}$ HSCs transfected with TOPFlash (Fig. 3F). These results collectively reinforce the conclusions that expression of exogenous L-Fabp in *L-Fabp*$^{-/-}$ HSCs rescues the ability of Plin5 to reverse HSC activation, elevate cellular lipid content, and regulate prolipogenic pathways. Furthermore, these effects appear to be independent of Plin2.

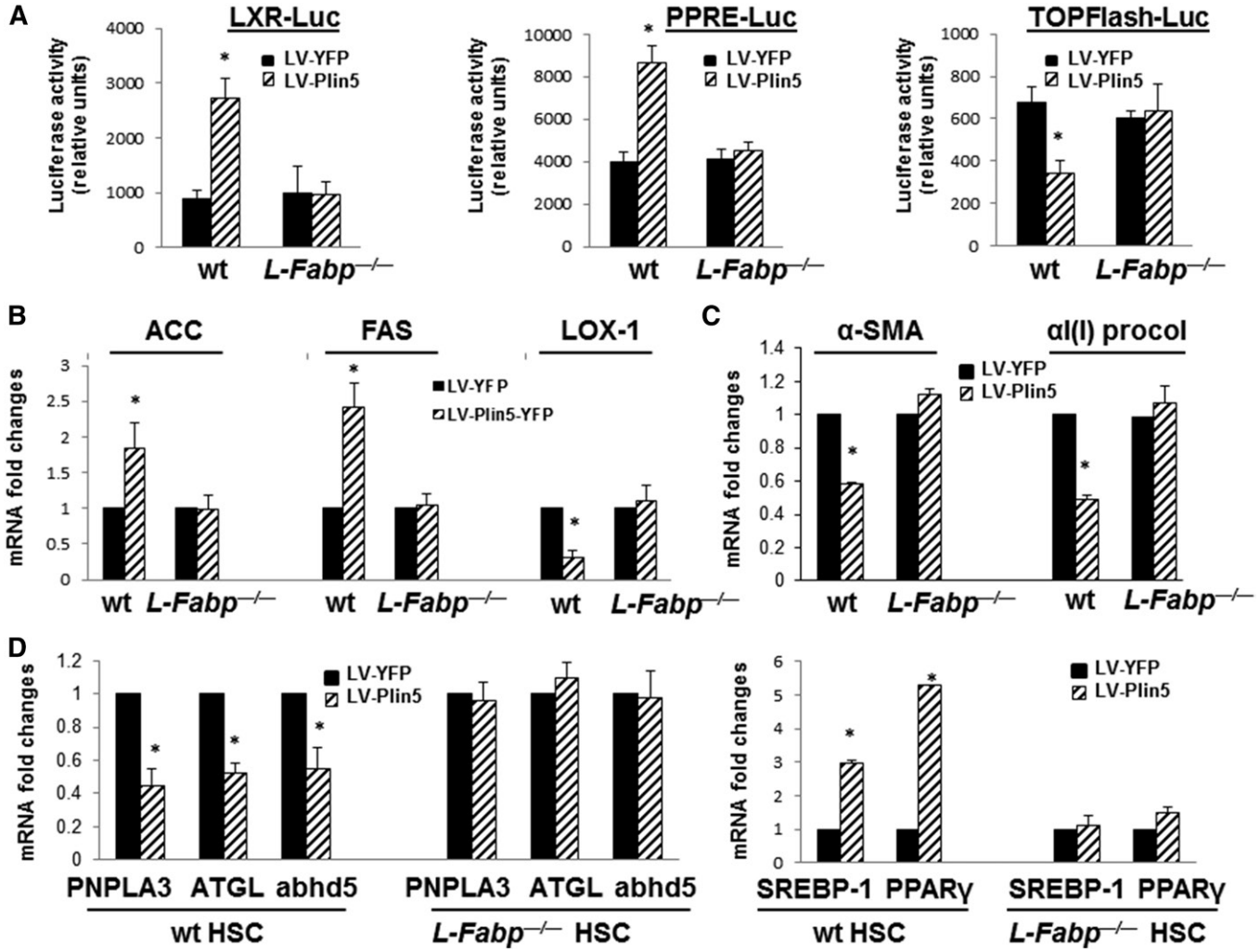

Fig. 2. L-Fabp is required for Plin5-mediated reversal of HSC activation and transcriptional induction of prolipogenic signaling pathways. Passaged WT or *L-Fabp*$^{-/-}$ HSCs were transduced with LV-Plin5-YFP or LV-YFP. After selection with puromycin, cells were prepared for experiments; *$P < 0.05$ vs. HSCs transduced with LV-YFP (corresponding solid columns). A: Luciferase activity assays of WT (wt) or *L-Fabp*$^{-/-}$ HSCs transduced with LV-Plin5-YFP or LV-YFP and followed by transfection with the luciferase reporter plasmids LXR-Luc, PPRE-Luc, or TOPFlash (n = 6). B: Real-time PCR analyses of downstream target genes of the signaling of SREBP-1 (ACC), PPARγ (FAS), and Wnt-1 (LOX-1). C: Real-time PCR analyses of genes relevant to HSC activation (n = 3). D: Real-time PCR analyses of genes relevant to lipolysis (left panel) and lipogenesis (right panel) (n = 3).

Expression of other FABPs in *L-Fabp*$^{-/-}$ HSCs rescues the ability of Plin5 to restore LD formation

Consistent with the findings above, lentiviral Plin5 restored LD formation in WT HSCs with Ad-LacZ or with Ad-L-Fabp, suggesting that endogenous expression of L-Fabp is sufficient for these effects in WT HSCs. However, LDs were only restored in lentivirally transduced Plin5 *L-Fabp*$^{-/-}$ HSCs transfected with Ad-L-Fabp, but not with Ad-LacZ (the lower right panel with arrow of the lower four panels in **Fig. 4A**). We previously observed that other FABPs were expressed in quiescent HSCs, albeit at very low levels relative to L-Fabp (18). To address the question whether other FABPs could replace L-Fabp in Plin5-mediated rescue of LD formation, WT and *L-Fabp*$^{-/-}$ HSCs were sequentially transduced with LV-Plin5-YFP or LV-YFP followed by recombinant adenoviral intestinal Fabp (Ad-I-Fabp), adipocyte Fabp (Ad-A-Fabp), or Ad-LacZ transduction (Fig. 4B). We found that either Ad-I-Fabp or Ad-A-Fabp together with Plin5 restored LDs in *L-Fabp*$^{-/-}$ HSCs (panels with arrows in Fig. 4C). In addition, and as found with the Ad-L-Fabp transduction experiments reported above, neither Ad-I-Fabp or Ad-A-Fabp transduction alone in *L-Fabp*$^{-/-}$ HSCs restored LD formation (Fig. 4 C). These findings again point to a role for endogenous L-Fabp in LD formation in response to Plin5 transduction in WT HSCs. Although we did not systematically examine the entire range of FABPs, our results suggest that the expression of exogenous L-Fabp as well as other FABPs effectively rescues the ability of Plin5 to restore LD formation in *L-Fabp*$^{-/-}$ HSCs.

Small molecule inhibitors of L-Fabp impair the ability of Plin5 to restore LD formation in HSCs

To address how Plin5 induces LD formation through an L-Fabp-dependent mechanism, we were guided by the finding that exogenous Plin5 significantly increased mRNA

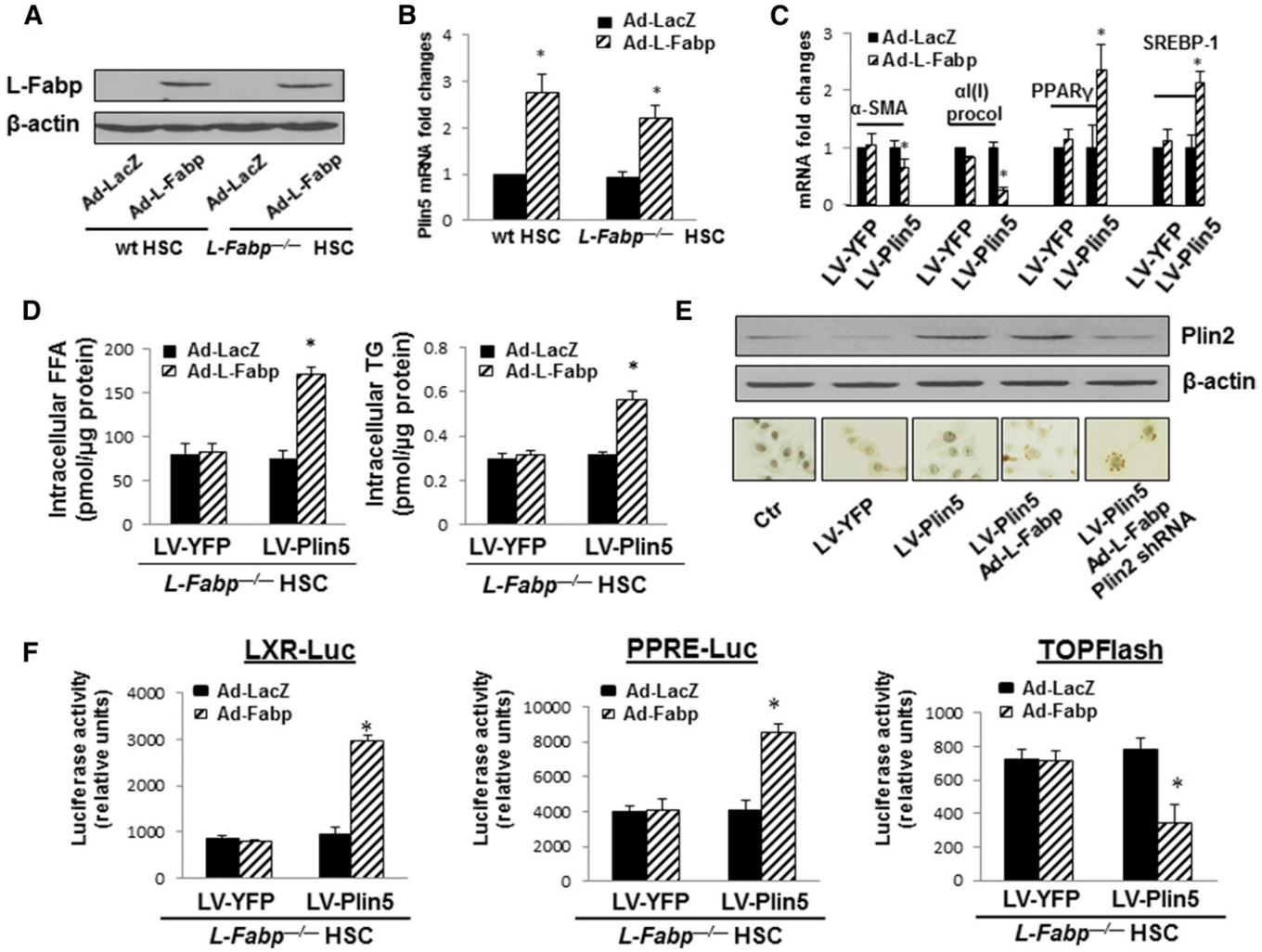

Fig. 3. Introduction of L-Fabp into *L-Fabp*$^{-/-}$HSCs rescues Plin5-mediated reversal of activation and prolipogenic activity. *L-Fabp*$^{-/-}$HSCs were transduced with LV-Plin5-YFP or LV-YFP, and in some experiments with Plin2 shRNA, then transduced with recombinant adenoviral Ad-L-Fabp or the control recombinant adenoviral Ad-LacZ. Twenty-four hours later, cells were prepared for experiments; *$P < 0.05$ vs. HSCs transduced with Ad-LacZ (corresponding solid columns). A: Western blotting analyses of L-Fabp in WT (wt) HSC or *L-Fabp*$^{-/-}$HSCs transducted with Ad-L-Fabp or Ad-LacZ, respectively. β-actin was an internal control for equal loading. Representative views of three independent tests are presented. B: Real-time PCR analyses of Plin5 in WT HSC and *L-Fabp*$^{-/-}$HSCs transducted with Ad-L-Fabp or Ad-LacZ (n = 3). C: Real-time PCR analyses of genes (n = 3). D: Analyses of cellular FFA and TG (n = 3). E: Western blotting analyses of the inhibitory efficiency of shRNAPlin2 and Oil Red O staining. Representative views from three independent experiments are presented. F: Luciferase activity assays of the transduced HSCs transfected with the luciferase reporter plasmids LXR-Luc, PPRE-Luc, or TOPFlash (n = 6).

abundance of endogenous L-Fabp in WT HSCs (**Fig. 5A**), and the transcriptional reporter GFP in our GFP-knockin *L-Fabp*$^{-/-}$ HSCs (17) (Fig. 5A). Further studies indicated that the expression of exogenous Plin5 had no apparent impact on mRNA expression of other FABPs in activated WT HSCs (Fig. 5B). These findings further reinforce the concept that endogenous L-Fabp induction may be a key step in the Plin5-mediated restoration of LDs in WT HSCs. To examine this possibility directly, we turned to a series of small molecule inhibitors of L-Fabp function engineered with varying degrees of specificity and potency (supplemental Fig. S1).

We focused on the most selective L-Fabp inhibitor (NSOP00313, abbreviated as NSOP313) at increasing doses in WT HSCs for 24 h before and after transduction with LV-Plin5-YFP. We found that treatment with NSOP313 caused a dose-dependent decrease in the formation of LDs (Fig. 5C), along with decreased cellular FFA and TG content (Fig. 5E). Moreover, higher doses of NSOP313 triggered upregulation of mRNAs associated with HSC activation and decreased expression of PPARγ mRNA (Fig. 5D).

We also asked whether the effects of Ad-L-Fabp in increasing endogenous Plin5 expression (see Fig. 3B) might be reversed following L-Fabp inhibitor treatment. Accordingly, NSOP313 at increasing doses was used to treat Ad-L-Fabp transduced WT HSCs, the data showing a dose-dependent reduction in Plin5 mRNA expression (Fig. 5F). These results together confirm the critical role of L-Fabp in regulating Plin5 in inhibiting HSC activation, increasing cellular lipid content, and restoring LD formation in HSCs.

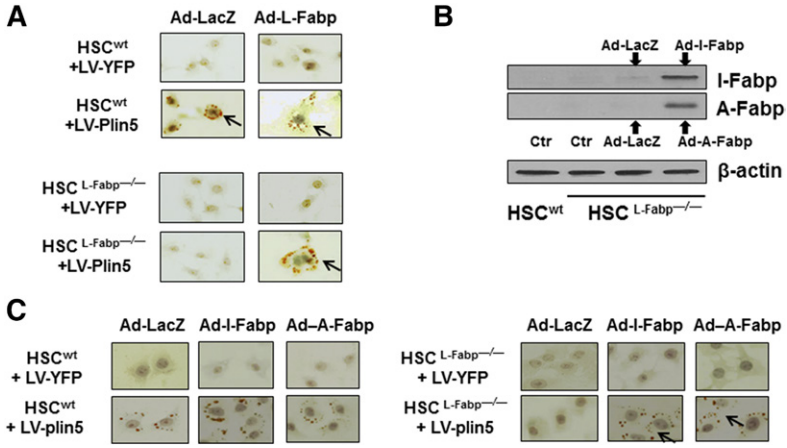

Fig. 4. Expression of other FABPs in *L-Fabp*$^{-/-}$HSCs rescues the ability of Plin5 to restore LD formation. Passaged WT (wt) or *L-Fabp*$^{-/-}$HSCs were transduced with LV-Plin5-YFP or LV-YFP, respectively. After selection with puromycin, cells were transduced with Ad-L-Fabp or Ad-LacZ (A and B) or were transduced with a recombinant adenovirus expressing I-Fabp (Ad-I-Fabp) or A-Fabp (Ad-A-Fabp) (C). Representative views from three independent experiments are presented. A: Oil Red O staining of LDs in HSCs transduced with Ad-L-Fabp or Ad-LacZ. B: Western blotting analyses of I-Fabp or A-Fabp. C: Oil Red O staining of LDs in HSCs transduced with Ad-I-Fabp, Ad-A-Fabp, or Ad-LacZ.

AMPK activation is required for L-Fabp-mediated Plin5-dependent restoration of lipogenesis and quiescence in *L-Fabp*$^{-/-}$ HSCs

We previously reported that exogenous Plin5 stimulated AMPK activation in WT HSCs, which in turn induced the expression of endogenous Plin5, a pathway required for restoring LD formation and inhibiting HSC activation (8). To address the role of AMPK activation in the coordination of L-Fabp with Plin5, we first explored the requirement of L-Fabp in the activation of AMPK by Plin5 in *L-Fabp*$^{-/-}$ HSCs. As shown in **Fig. 6A**, forced expression of exogenous Plin5 increased the abundance of phosphorylated AMPK in both WT and *L-Fabp*$^{-/-}$ HSCs. By contrast, forced expression of L-Fabp alone could not activate AMPK in *L-Fabp*$^{-/-}$ HSCs (Fig. 6A). These findings suggest that L-Fabp is not required for Plin5 to activate AMPK in HSCs. They also suggest that the introduction of Ad-L-Fabp alone into *L-Fabp*$^{-/-}$ HSCs is not sufficient for AMPK activation. We further studied *L-Fabp*$^{-/-}$ HSCs transduced with LV-Plin5-YFP or LV-YFP and subsequent Ad-L-Fabp rescue, followed by treatment with the selective AMPK inhibitor Compound C at 20 μM for 24 h. AMPK inhibition significantly attenuated the effects of Plin5 and L-Fabp on regulating expression of genes relevant to HSC activation, lipogenesis, and lipolysis in *L-Fabp*$^{-/-}$ HSCs (Fig. 6B) and also attenuated LD formation (Fig. 6C). Additionally, AMPK inhibition dose-dependently reversed Plin5-dependent increases in endogenous L-Fabp mRNA in WT HSCs (Fig. 6D). These findings suggest that Plin5-induced expression of endogenous L-Fabp in HSCs is likely AMPK-dependent. AMPK inhibition also reversed the transcriptional programs of lipogenic induction of LXR and PPARγ and of Wnt suppression as indicated by the luciferase assays using reporter constructs outlined above (Fig. 6E). Taken together, these results strongly suggest that AMPK activation is required for the coordination of L-Fabp with Plin5 in mediating rescue of quiescence in *L-Fabp*$^{-/-}$ HSCs.

DISCUSSION

We recently reported that the activation of HSCs was temporally coincident with the loss of LDs, the depletion of Plin5 (8), and the suppression of L-Fabp expression (18) both in vitro and in vivo. The current findings extend those observations by demonstrating that exogenous Plin5 induces endogenous L-Fabp expression in WT HSCs, suggesting a requirement for L-Fabp in the rescue of quiescence mediated by Plin5. We further show that either lifelong absence of L-Fabp (in *L-Fabp*$^{-/-}$ HSCs) or pharmacologic inhibition of endogenous L-Fabp in WT HSCs abrogated the ability of Plin5 to reverse HSC activation and also eliminated LD formation and lipid accumulation. Conversely, adenoviral-mediated expression of exogenous L-Fabp in *L-Fabp*$^{-/-}$ HSCs rescued the ability of Plin5 to restore quiescence. Accordingly, a central conclusion of this work is that L-Fabp is required for Plin5-mediated rescue of cellular quiescence in HSCs, through pathways that intersect with the induction of lipogenic gene programs. That being said, we recognize that the range of functions of Plin5 implied from studies in animal models is still controversial (9, 41).

Accumulating evidence has shown the importance of cellular lipids in maintaining HSCs in a state of quiescence, although the precise roles of key LD proteins remain elusive. At the molecular level, independent work strongly supports the idea that Plin5 functions as a scaffold for three major key lipolytic players, abhd5, ATGL, and hormone-sensitive lipase, in hydrolysis of TG in LDs (42–45). Plin5 is highly expressed in oxidative tissues such as skeletal muscle, liver, and heart and is central to lipid homeostasis in these tissues. Studies in cell systems have ascribed several metabolic roles to Plin5 and demonstrated interactions with other proteins that are requisite for these functions (41). Our results support an important role for Plin5 in elevating cellular lipid content in HSCs (8); namely, induction of lipogenic pathways through transcriptional activation of SREBP and PPARγ dependent pathways. We recognize that further studies will be required to explore the precise mechanisms of increased de novo lipogenesis observed.

Studies suggest that lecithin-retinol acyltransferase (LRAT) acts as the sole retinol acyltransferase in the liver and is responsible for the formation of retinyl esters in HSCs (46). LRAT is highly expressed in quiescent HSCs and downregulated during HSC activation (47). Lrat $^{-/-}$

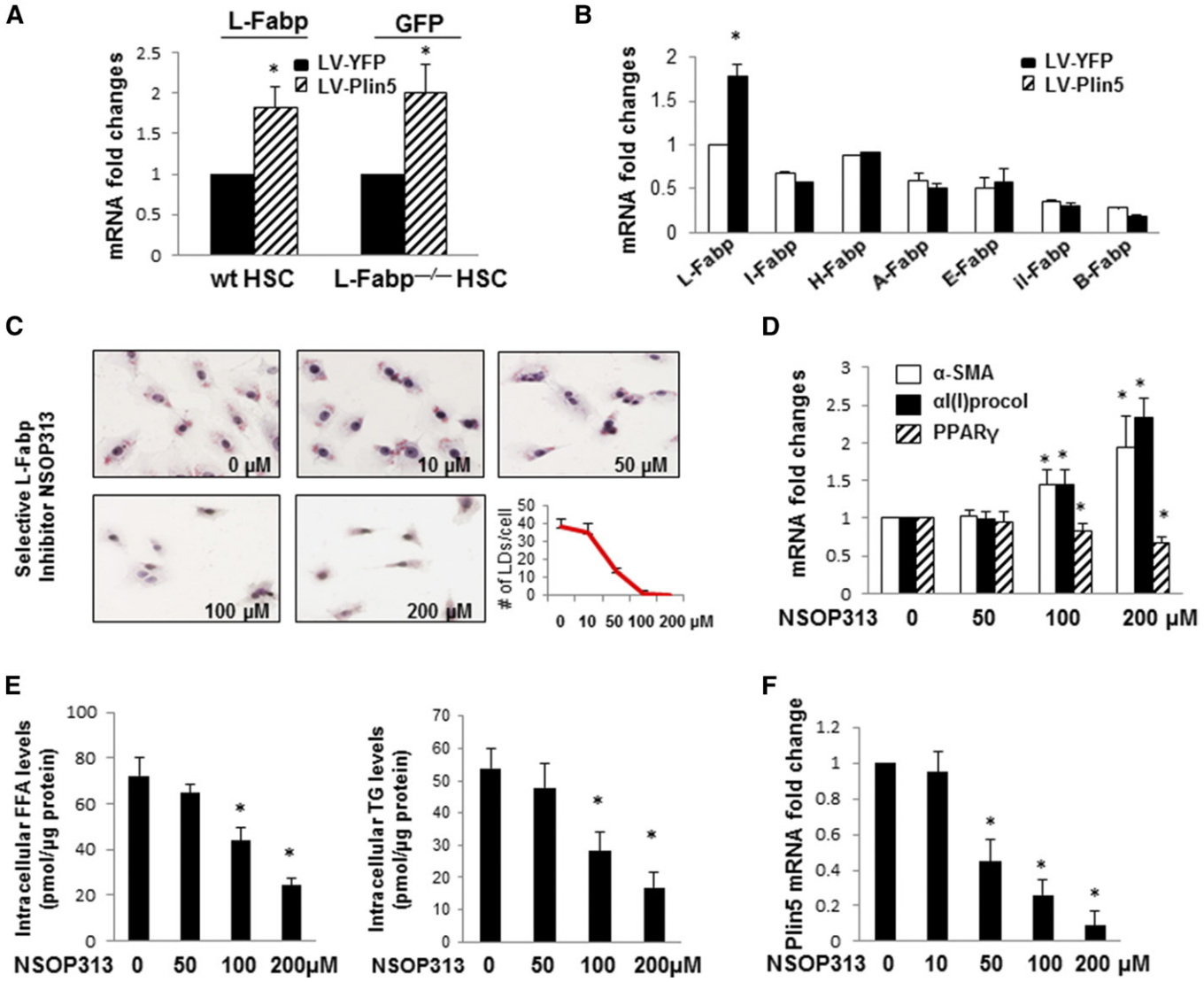

Fig. 5. Small molecule inhibitors of L-Fabp impede the ability of Plin5 to restore LD formation in HSCs. A: Passaged WT (wt) HSCs or *L-Fabp*$^{-/-}$ HSCs were transduced with LV-Plin5-YFP or LV-YFP. Total RNA was prepared for real-time PCR analyses; *$P < 0.05$ vs. HSCs transduced with LV-YFP (corresponding solid columns) (n = 3). B: Real-time PCR analyses of WT HSCs transduced with LV-Plin5-YFP or LV-YFP. All data were normalized to the expression of L-Fabp in HSCs with LV-YFP; *$P < 0.05$ vs. HSCs transduced with LV-YFP (corresponding solid columns) (n = 3). C–E: WT HSCs were transduced with LV-Plin5-YFP followed by treatment with the selective L-Fabp inhibitor NSOP00313 (referred to as NSOP313 in text) at the indicated doses for 24 h. C: Oil Red O staining of cellular LDs (Representative views from three independent experiments are presented) and the numbers of LDs per cell (mean from 10 cells). D: Real-time PCR analyses; *$P < 0.05$ vs. HSCs without NSOP313 treatment (n = 3). E: Analyses of cellular FFA and TG content. *$P < 0.05$ vs. HSCs without NSOP313 treatment (n = 3). F: Real-time PCR analyses of endogenous Plin5 mRNA in Ad-L-Fabp transduced WT HSCs with treatment of NSOP313 at the indicated doses. *$P < 0.05$ vs. HSCs without NSOP313 treatment.

mice showed a striking total absence of large lipid-containing droplets that normally store hepatic retinoid within HSCs (48). However, the absence of retinyl ester-containing LDs does not promote either spontaneous HSC activation, or worsen bile duct ligation-induced or carbon tetrachloride-induced liver fibrosis (47). Our earlier studies showed that exogenous Plin5 had no impact on the expression of endogenous LRAT in WT HSCs (8). We considered the possibility that Plin5 and L-Fabp transduction might modify retinol content of HSCs but our findings demonstrated only very low levels of retinol with no differences by genotype and retinyl esters were undetectable (supplemental Table S1). Because these studies were undertaken in passaged HSCs, those findings would be predicted.

Our findings also highlight a potential functional redundancy in the FABP requirement for Plin5-dependent rescue of quiescence and LD formation. We have previously shown that among all FABPs, L-Fabp is by far the most abundantly expressed member in quiescent HSCs (18). Other FABP members in quiescent HSCs are either expressed at a very low level or their expression is unchanged during HSC activation (18). We observed that exogenous Plin5 in WT HSCs induced endogenous L-Fabp expression, but not other FABP members (Fig. 5B), suggesting specificity in Plin5-dependent effects via L-Fabp in promoting LD

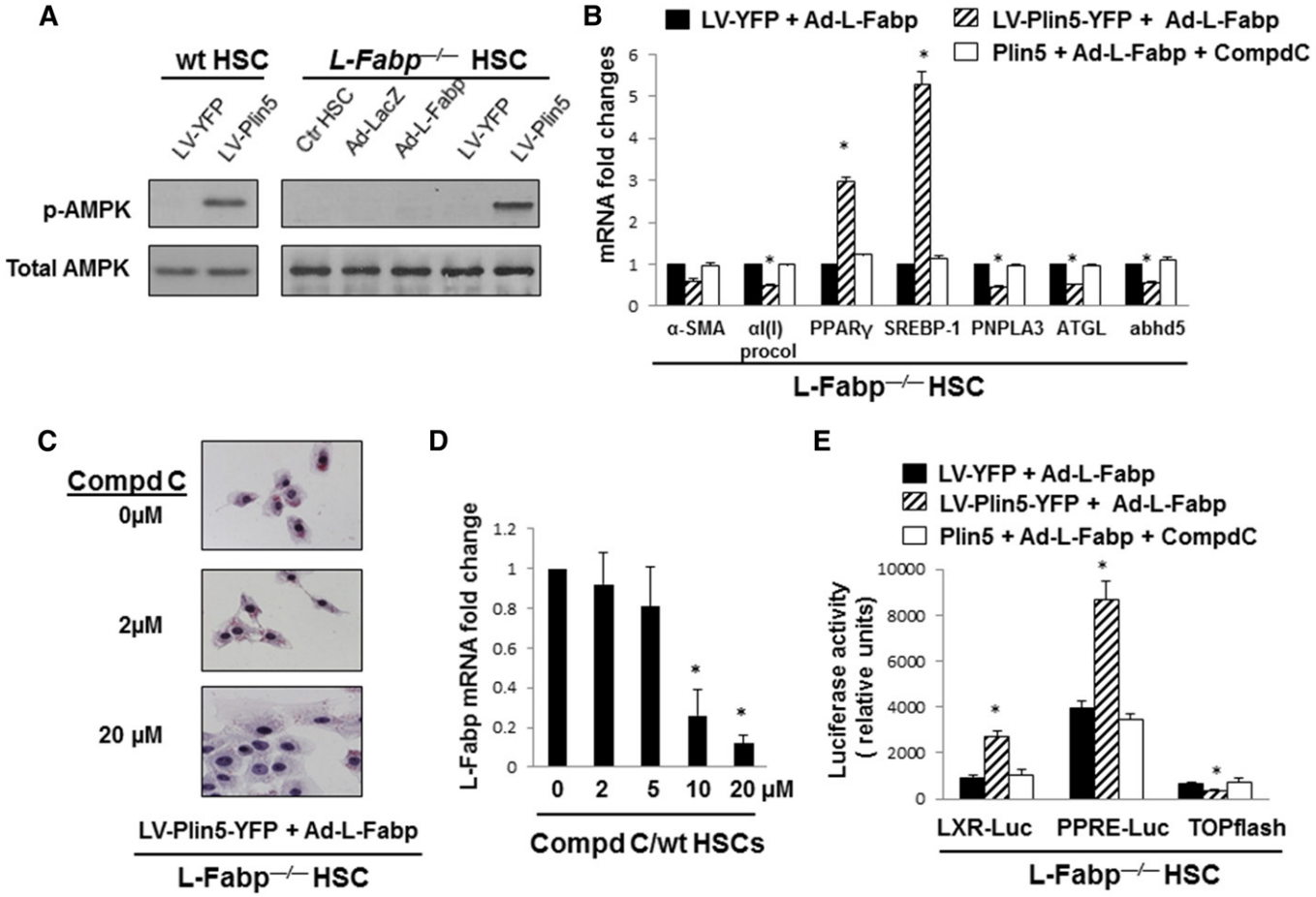

Fig. 6. AMPK activation is required for L-Fabp-dependent Plin5-mediated restoration of lipogenesis and quiescence in *L-Fabp*$^{-/-}$ HSCs. A: Western blotting analyses of phosphorylated AMPK (p-AMPK) in WT HSCs or in *L-Fabp*$^{-/-}$ HSCs transduced with recombinant virus as indicated. Total AMPK abundance was used as an internal control for equal loading. Representative views from 3 independent experiments are presented; (B, C, and E). *L-Fabp*$^{-/-}$ HSCs were sequentially transduced with LV-Plin5-YFP or LV-YFP, and then with Ad-L-Fabp, followed by treatment with the AMPK inhibitor Compound C (CompdC), at the indicated concentrations. B: Real-time PCR analyses (n = 3); *$P < 0.05$ vs. HSCs transduced with LV-YFP (corresponding solid columns). C: Oil Red O staining of cellular LDs. Representative views from three independent experiments are presented. D: Real-time PCR analyses of endogenous L-Fabp in WT HSC transduced with LV-Plin5 (n = 3); *$P <$ 0.05 vs. HSCs with no CompdC. E: Luciferase activity assays of the transduced HSCs transfected with the luciferase reporter plasmids LXR-Luc, PPRE-Luc, or TOPFlash (n = 6).

formation and restoration of quiescence. On the other hand, our findings also suggest that L-Fabp is not functionally unique and its role could be replicated by other FABPs, including I-Fabp or A-Fabp. Although we did not undertake a comprehensive evaluation of the entire FABP family, it is tempting to speculate that under circumstances where other FABPs might be induced (not examined here), there may yet be L-Fabp-independent pathways of restoring quiescence. Along these lines, whereas we found that the most specific and potent small molecule L-Fabp inhibitor (NSOP313) effectively replicated the phenotypes observed with *L-Fabp* deletion (Fig. 5), we also found that other L-Fabp inhibitors (supplemental Fig. S1) showed similar effects but were either less selective or more toxic.

Our earlier work suggested that germline *L-Fabp* deletion functions to attenuate high-fat, fibrogenic, diet-induced hepatic steatosis and fibrosis, raising the possibility that inhibition of L-Fabp might be a feasible strategy to mitigate the effects of hepatic steatosis and necroinflammatory disease progression. However, it bears emphasis that L-Fabp is abundantly expressed in hepatocytes as well as in HSCs and it is possible that its roles and functions are exerted in a distinct cell- and metabolic-state-specific context. The current findings support the concept of this cell-type-specific function by demonstrating that genetic deletion or pharmacologic inhibition of L-Fabp essentially eliminates the ability of Plin5 to restore LD formation in either WT or *L-Fabp*$^{-/-}$ HSCs. The findings from these in vitro studies additionally suggest that pharmacologic inhibition of L-Fabp, by mitigating LD formation and induction of a lipogenic program, might simultaneously induce HSC activation.

An overarching question in our approach relates to whether the expression levels of exogenous Plin5 are reflective of those encountered physiologically. We demonstrated that Plin5 protein is indeed detectable in freshly isolated HSCs, albeit at levels somewhat lower than those seen with forced lentiviral expression in passaged HSCs (Fig. 1C, D). In addition, we previously reported that transduction of WT HSCs with LV-Plin5-YFP or the empty

control virus LV-YFP shows significant differences in inhibiting HSC activation (8). Introduction of LV-Plin5-YFP, but not LV-YFP, significantly reduces cell growth and expression of activation-relevant genes and restores LD formation in HSCs. Additionally, we showed that the major functional domain of Plin5 for the LD formation in HSCs resided in a domain spanning amino acids 1–188 (aa1–188) of Plin5 (8) and that overexpression of a subdomain of Plin5 (aa189–463) had no function in LD formation. These prior results, coupled with the new findings shown in Fig. 1C and D, greatly diminish the possibility of a neomorphic phenotype of Plin5 transduction or of an artifact derived from nonspecific recombinant lentiviral transduction.

It was reported that introduction of Plin2 promotes downregulation of HSC activation and is functionally linked to the expression of fibrogenic genes (40). We observed that forced expression of Plin5 was coupled with the expression of endogenous Plin2 in HSCs (Fig. 1E). Inhibition of the Plin2 expression by Plin2 shRNA showed no impact on the Plin5 function in restoring LD in HSCs (Fig. 3E). Our results and others suggest that Plin5, Plin2, or even other lipid droplet proteins, could independently function in HSCs.

Plin5 was reported to be phosphorylated by protein kinase A (PKA) (49–51), and the serine at 155 in Plin5 has been proposed as the PKA phosphorylation site (50). Phosphorylation of Plin5 by PKA stimulated the interaction of Plin5 and ATGL (51), which might play a critical role in Plin5-regulated lipolysis (50). Plin5 has been proposed to be an important molecular link that couples the coordinated catecholamine activation of the PKA pathway and of lipid droplet lipolysis with transcriptional regulation to promote efficient fatty acid catabolism (49). The possibility that Plin5 modulates lipid hydrolysis in HSCs and the role, if any, for L-Fabp will require further study.

AMPK is a well-conserved serine/threonine-protein kinase, which acts as a cellular energy and nutrient sensor and plays a crucial role in regulation of metabolic pathways and cellular energy homeostasis (52). Phosphorylation of AMPK at Thr-172 stimulates its kinase activity (53). AMPK acts as an anti-lipolytic factor by phosphorylating and inactivating hormone-sensitive lipase (54) and blocking its translocation to LDs (55). We previously showed that the activation of AMPK increased cellular TG in HSCs and inhibited activation (29). We also showed that PKA and AMPK played opposite roles in regulating HSC activation (56). In the current study, we observed that activation of AMPK played a key role in the coordination of L-Fabp with Plin5 in inhibiting HSC activation and restoring LD formation. Our findings lead us to hypothesize that a positive-feedback loop exists between Plin5 and AMPK activation in HSCs in which expression of Plin5 results in activation of AMPK and induction of pro-lipogenic genes (**Fig. 7**).

Our results also suggest that forced expression of Plin5 stimulated AMPK activation in WT and *L-Fabp*$^{-/-}$ HSCs. However, overexpression of exogenous L-Fabp alone could not activate AMPK. These results suggest that AMPK might be a downstream target of Plin5, and upstream of L-Fabp (i.e., Plin5 → AMPK activation → L-Fabp; not Plin5 → L-Fabp → AMPK activation). This suggestion is supported by experiments showing that, although forced expression of Plin5 induced expression of endogenous L-Fabp in WT HSCs (Fig. 5A), inhibition of Plin5 signaling by AMPK inhibition dose-dependently reduced L-Fabp expression. These findings beg the question of whether AMPK activation modulates L-Fabp expression, which is a subject of future investigation.

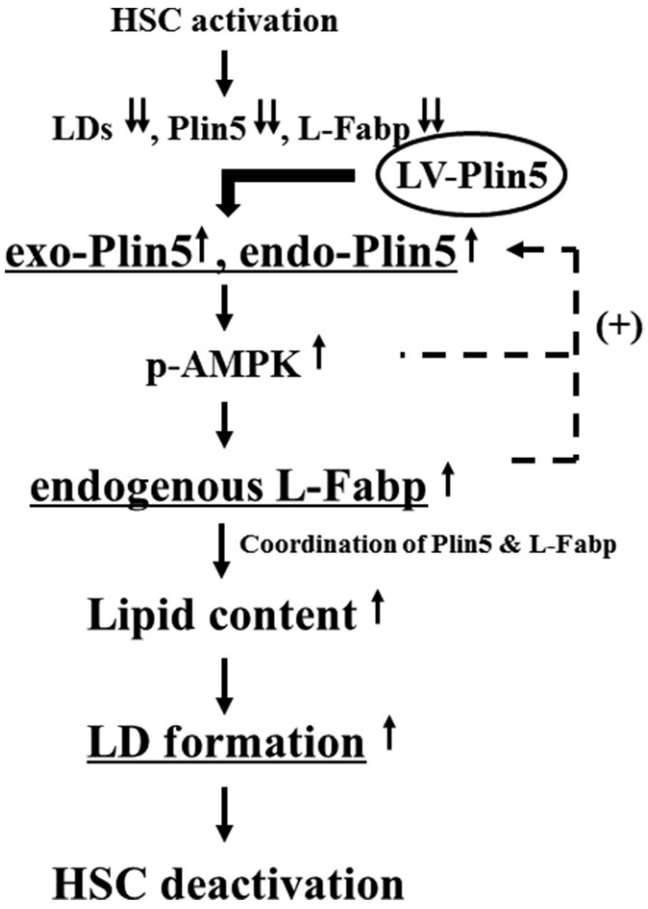

Fig. 7. Summary overview of the proposed pathways explored in this report. Stellate cell (HSC) activation is temporally accompanied by loss of lipid droplets (LDs) along with decreased expression of both Plin5 and L-Fabp. Lentiviral (LV) transduction of Plin5 into WT HSCs restores exogenous (exo) Plin5, leading to AMPK activation and increased endogenous L-Fabp expression which in combination further increases endogenous (endo) Plin5 expression. The coordination of Plin5 and L-Fabp promotes lipid (fatty acid) uptake and increases lipogenesis, leading to the elevation of cellular lipid content. Upregulation of endogenous L-Fabp is a requisite step in this pathway, the net effects leading to accumulation of LDs and a return to quiescence with HSC deactivation.

Forced expression of L-Fabp elevated the mRNA level of endogenous Plin5 by 2- to 3-fold in both WT HSCs and in *L-Fabp*$^{-/-}$ HSCs (Fig. 3B), consistent with our prior observations (18). However, forced expression of exogenous L-Fabp itself did not inhibit expression of HSC activation-relevant genes (Fig. 3C), augment cellular lipid content (Fig. 3D), nor rescue LD formation in *L-Fabp*$^{-/-}$ HSCs (Fig. 4A). These observations imply that despite the ability of forced L-Fabp expression to increase endogenous Plin5 mRNA by 2- to 3-fold, the levels of Plin5 protein remain

below the threshold necessary for complete rescue of quiescence as previously observed in WT HSCs (18). In addition, as noted above, the introduction of Ad-L-Fabp alone into *L-Fabp*$^{-/-}$ HSCs failed to activate AMPK. Based on the collective observations presented above, a simplified model is proposed to address the role of AMPK and L-Fabp in mediating/coordinating the effects of Plin5 in restoring HSC quiescence (Fig. 7). It bears emphasis that this model does not exclude other pathways by which L-Fabp functions in coordinating with Plin5 the inhibition of HSC activation. In summary, our results demonstrate that L-Fabp plays a critical role in coordinating with Plin5 in modulating expression of lipogenic genes, restoring LD formation, elevating lipid content, and inhibiting HSC activation.

REFERENCES

1. Puche, J. E., Y. Saiman, and S. L. Friedman. 2013. Hepatic stellate cells and liver fibrosis. *Compr. Physiol.* **3:** 1473–1492.
2. Friedman, S. L. 2015. Hepatic fibrosis: emerging therapies. *Dig. Dis.* **33:** 504–507.
3. Koyama, Y., and D. A. Brenner. 2017. Liver inflammation and fibrosis. *J. Clin. Invest.* **127:** 55–64.
4. Kimmel, A. R., and C. Sztalryd. 2016. The perilipins: major cytosolic lipid droplet-associated proteins and their roles in cellular lipid storage, mobilization, and systemic homeostasis. *Annu. Rev. Nutr.* **36:** 471–509.
5. Carr, R. M., and R. S. Ahima. 2016. Pathophysiology of lipid droplet proteins in liver diseases. *Exp. Cell Res.* **340:** 187–192.
6. Conte, M., C. Franceschi, M. Sandri, and S. Salvioli. 2016. Perilipin 2 and age-related metabolic diseases: a new perspective. *Trends Endocrinol. Metab.* **27:** 893–903.
7. MacPherson, R. E., and S. J. Peters. 2015. Piecing together the puzzle of perilipin proteins and skeletal muscle lipolysis. *Appl. Physiol. Nutr. Metab.* **40:** 641–651.
8. Lin, J., and A. Chen. 2016. Perilipin 5 restores the formation of lipid droplets in activated hepatic stellate cells and inhibits their activation. *Lab. Invest.* **96:** 791–806.
9. Wang, C., Y. Zhao, X. Gao, L. Li, Y. Yuan, F. Liu, L. Zhang, J. Wu, P. Hu, X. Zhang, et al. 2015. Perilipin 5 improves hepatic lipotoxicity by inhibiting lipolysis. *Hepatology.* **61:** 870–882.
10. Tsukamoto, H., H. She, S. Hazra, J. Cheng, and T. Miyahara. 2006. Anti-adipogenic regulation underlies hepatic stellate cell transdifferentiation. *J. Gastroenterol. Hepatol.* **21(Suppl 3):** S102–S105.
11. Tsukamoto, H., H. She, S. Hazra, J. Cheng, and J. Wang. 2008. Fat paradox of steatohepatitis. *J. Gastroenterol. Hepatol.* **23(Suppl 1):** S104–S107.
12. Yamamoto, T., A. Yamamoto, M. Watanabe, T. Matsuo, N. Yamazaki, M. Kataoka, H. Terada, and Y. Shinohara. 2009. Classification of FABP isoforms and tissues based on quantitative evaluation of transcript levels of these isoforms in various rat tissues. *Biotechnol. Lett.* **31:** 1695–1701.
13. Newberry, E. P., S. M. Kennedy, Y. Xie, J. Luo, and N. O. Davidson. 2009. Diet-induced alterations in intestinal and extrahepatic lipid metabolism in liver fatty acid binding protein knockout mice. *Mol. Cell. Biochem.* **326:** 79–86.
14. Newberry, E. P., S. M. Kennedy, Y. Xie, B. T. Sternard, J. Luo, and N. O. Davidson. 2008. Diet-induced obesity and hepatic steatosis in L-Fabp / mice is abrogated with SF, but not PUFA, feeding and attenuated after cholesterol supplementation. *Am. J. Physiol. Gastrointest. Liver Physiol.* **294:** G307–G314.
15. Newberry, E. P., Y. Xie, S. Kennedy, X. Han, K. K. Buhman, J. Luo, R. W. Gross, and N. O. Davidson. 2003. Decreased hepatic triglyceride accumulation and altered fatty acid uptake in mice with deletion of the liver fatty acid-binding protein gene. *J. Biol. Chem.* **278:** 51664–51672.
16. Newberry, E. P., Y. Xie, S. M. Kennedy, M. J. Graham, R. M. Crooke, H. Jiang, A. Chen, D. S. Ory, and N. O. Davidson. 2017. Prevention of hepatic fibrosis with liver microsomal triglyceride transfer protein deletion in liver fatty acid binding protein null mice. *Hepatology.* **65:** 836–852.
17. Newberry, E. P., Y. Xie, S. M. Kennedy, J. Luo, and N. O. Davidson. 2006. Protection against Western diet-induced obesity and hepatic steatosis in liver fatty acid-binding protein knockout mice. *Hepatology.* **44:** 1191–1205.
18. Chen, A., Y. Tang, V. Davis, F. F. Hsu, S. M. Kennedy, H. Song, J. Turk, E. M. Brunt, E. P. Newberry, and N. O. Davidson. 2013. Liver fatty acid binding protein (L-Fabp) modulates murine stellate cell activation and diet induced nonalcoholic fatty liver disease. *Hepatology.* **57:** 2202–2212.
19. Fu, Y., S. Zheng, J. Lin, J. Ryerse, and A. Chen. 2008. Curcumin protects the rat liver from CCl4-caused injury and fibrogenesis by attenuating oxidative stress and suppressing inflammation. *Mol. Pharmacol.* **73:** 399–409.
20. Kane, C. D., and D. A. Bernlohr. 1996. A simple assay for intracellular lipid-binding proteins using displacement of 1-anilinonaphthalene 8-sulfonic acid. *Anal. Biochem.* **233:** 197–204.
21. Lin, J., Y. Tang, Q. Kang, and A. Chen. 2012. Curcumin eliminates the inhibitory effect of advanced glycation end-products (AGEs) on gene expression of AGE receptor-1 in hepatic stellate cells in vitro. *Lab. Invest.* **92:** 827–841.
22. Schmittgen, T. D., B. A. Zakrajsek, A. G. Mills, V. Gorn, M. J. Singer, and M. W. Reed. 2000. Quantitative reverse transcription-polymerase chain reaction to study mRNA decay: comparison of endpoint and real-time methods. *Anal. Biochem.* **285:** 194–204.
23. Hall, A. M., B. M. Wiczer, T. Herrmann, W. Stremmel, and D. A. Bernlohr. 2005. Enzymatic properties of purified murine fatty acid transport protein 4 and analysis of acyl-CoA synthetase activities in tissues from FATP4 null mice. *J. Biol. Chem.* **280:** 11948–11954.
24. Lin, J., Y. Tang, Q. Kang, Y. Feng, and A. Chen. 2012. Curcumin inhibits gene expression of receptor for advanced glycation end-products (RAGE) in hepatic stellate cells in vitro by elevating PPARgamma activity and attenuating oxidative stress. *Br. J. Pharmacol.* **166:** 2212–2227.
25. Zheng, S., and A. Chen. 2004. Activation of PPARgamma is required for curcumin to induce apoptosis and to inhibit the expression of extracellular matrix genes in hepatic stellate cells in vitro. *Biochem. J.* **384:** 149–157.
26. Steffensen, K. R., E. Holter, N. Alikhani, W. Eskild, and J. A. Gustafsson. 2003. Glucocorticoid response and promoter occupancy of the mouse LXRalpha gene. *Biochem. Biophys. Res. Commun.* **312:** 716–724.
27. DasGupta, R., A. Kaykas, R. T. Moon, and N. Perrimon. 2005. Functional genomic analysis of the Wnt-wingless signaling pathway. *Science.* **308:** 826–833.
28. Lin, J., S. Zheng, and A. Chen. 2009. Curcumin attenuates the effects of insulin on stimulating hepatic stellate cell activation by interrupting insulin signaling and attenuating oxidative stress. *Lab. Invest.* **89:** 1397–1409.
29. Tang, Y., and A. Chen. 2010. Curcumin protects hepatic stellate cells against leptin-induced activation in vitro by accumulating intracellular lipids. *Endocrinology.* **151:** 4168–4177.
30. D'Ambrosio, D. N., J. L. Walewski, R. D. Clugston, P. D. Berk, R. A. Rippe, and W. S. Blaner. 2011. Distinct populations of hepatic stellate cells in the mouse liver have different capacities for retinoid and lipid storage. *PLoS One.* **6:** e24993.
31. Friedman, S. L. 2008. Mechanisms of hepatic fibrogenesis. *Gastroenterology.* **134:** 1655–1669.
32. Laurencikiene, J., and M. Ryden. 2012. Liver X receptors and fat cell metabolism. *Int. J. Obes. (Lond.)* **36:** 1494–1502.
33. Loren, J., Z. Huang, B. A. Laffitte, and V. Molteni. 2013. Liver X receptor modulators: a review of recently patented compounds (2009–2012). *Expert Opin. Ther. Pat.* **23:** 1317–1335.
34. Santos, G. M., A. Neves Fde, and A. A. Amato. 2015. Thermogenesis in white adipose tissue: an unfinished story about PPARgamma. *Biochim. Biophys. Acta.* **1850:** 691–695.
35. Lecarpentier, Y., and A. Vallee. 2016. Opposite interplay between PPAR gamma and canonical Wnt/beta-catenin pathway in amyotrophic lateral sclerosis. *Front. Neurol.* **7:** 100.
36. Vallée, A., and Y. Lecarpentier. 2016. Alzheimer disease: crosstalk between the canonical Wnt/beta-catenin pathway and PPARs alpha and gamma. *Front. Neurosci.* **10:** 459.
37. Talukdar, S., and F. B. Hillgartner. 2006. The mechanism mediating the activation of acetyl-coenzyme A carboxylase-alpha gene transcription by the liver X receptor agonist T0–901317. *J. Lipid Res.* **47:** 2451–2461.
38. Musri, M. M., and M. Parrizas. 2012. Epigenetic regulation of adipogenesis. *Curr. Opin. Clin. Nutr. Metab. Care.* **15:** 342–349.

39. Kang, Q., and A. Chen. 2009. Curcumin eliminates oxidized LDL roles in activating hepatic stellate cells by suppressing gene expression of lectin-like oxidized LDL receptor-1. *Lab. Invest.* **89:** 1275–1290.
40. Lee, T. F., K. M. Mak, O. Rackovsky, Y. L. Lin, A. J. Kwong, J. C. Loke, and S. L. Friedman. 2010. Downregulation of hepatic stellate cell activation by retinol and palmitate mediated by adipose differentiation-related protein (ADRP). *J. Cell. Physiol.* **223:** 648–657.
41. Mason, R. R., and M. J. Watt. 2015. Unraveling the roles of PLIN5: linking cell biology to physiology. *Trends Endocrinol. Metab.* **26:** 144–152.
42. Granneman, J. G., H. P. Moore, E. P. Mottillo, and Z. Zhu. 2009. Functional interactions between Mldp (LSDP5) and Abhd5 in the control of intracellular lipid accumulation. *J. Biol. Chem.* **284:** 3049–3057.
43. Granneman, J. G., H. P. Moore, E. P. Mottillo, Z. Zhu, and L. Zhou. 2011. Interactions of perilipin-5 (Plin5) with adipose triglyceride lipase. *J. Biol. Chem.* **286:** 5126–5135.
44. Wolins, N. E., B. K. Quaynor, J. R. Skinner, A. Tzekov, M. A. Croce, M. C. Gropler, V. Varma, A. Yao-Borengasser, N. Rasouli, P. A. Kern, et al. 2006. OXPAT/PAT-1 is a PPAR-induced lipid droplet protein that promotes fatty acid utilization. *Diabetes.* **55:** 3418–3428.
45. Wang, H., and C. Sztalryd. 2011. Oxidative tissue: perilipin 5 links storage with the furnace. *Trends Endocrinol. Metab.* **22:** 197–203.
46. Blaner, W. S., S. M. O'Byrne, N. Wongsiriroj, J. Kluwe, D. M. D'Ambrosio, H. Jiang, R. F. Schwabe, E. M. Hillman, R. Piantedosi, and J. Libien. 2009. Hepatic stellate cell lipid droplets: a specialized lipid droplet for retinoid storage. *Biochim. Biophys. Acta.* **1791:** 467–473.
47. Kluwe, J., N. Wongsiriroj, J. S. Troeger, G. Y. Gwak, D. H. Dapito, J. P. Pradere, H. Jiang, M. Siddiqi, R. Piantedosi, S. M. O'Byrne, et al. 2011. Absence of hepatic stellate cell retinoid lipid droplets does not enhance hepatic fibrosis but decreases hepatic carcinogenesis. *Gut.* **60:** 1260–1268.
48. O'Byrne, S. M., N. Wongsiriroj, J. Libien, S. Vogel, I. J. Goldberg, W. Baehr, K. Palczewski, and W. S. Blaner. 2005. Retinoid absorption and storage is impaired in mice lacking lecithin:retinol acyltransferase (LRAT). *J. Biol. Chem.* **280:** 35647–35657.
49. Gallardo-Montejano, V. I., G. Saxena, C. M. Kusminski, C. Yang, J. L. McAfee, L. Hahner, K. Hoch, W. Dubinsky, V. A. Narkar, and P. E. Bickel. 2016. Nuclear perilipin 5 integrates lipid droplet lipolysis with PGC-1alpha/SIRT1-dependent transcriptional regulation of mitochondrial function. *Nat. Commun.* **7:** 12723.
50. Pollak, N. M., D. Jaeger, S. Kolleritsch, R. Zimmermann, R. Zechner, A. Lass, and G. Haemmerle. 2015. The interplay of protein kinase A and perilipin 5 regulates cardiac lipolysis. *J. Biol. Chem.* **290:** 1295–1306.
51. Wang, H., M. Bell, U. Sreenivasan, H. Hu, J. Liu, K. Dalen, C. Londos, T. Yamaguchi, M. A. Rizzo, R. Coleman, et al. 2011. Unique regulation of adipose triglyceride lipase (ATGL) by perilipin 5, a lipid droplet-associated protein. *J. Biol. Chem.* **286:** 15707–15715.
52. Fisslthaler, B., and I. Fleming. 2009. Activation and signaling by the AMP-activated protein kinase in endothelial cells. *Circ. Res.* **105:** 114–127.
53. Suter, M., U. Riek, R. Tuerk, U. Schlattner, T. Wallimann, and D. Neumann. 2006. Dissecting the role of 5′-AMP for allosteric stimulation, activation, and deactivation of AMP-activated protein kinase. *J. Biol. Chem.* **281:** 32207–32216.
54. Garton, A. J., and S. J. Yeaman. 1990. Identification and role of the basal phosphorylation site on hormone-sensitive lipase. *Eur. J. Biochem.* **191:** 245–250.
55. Daval, M., F. Diot-Dupuy, R. Bazin, I. Hainault, B. Viollet, S. Vaulont, E. Hajduch, P. Ferre, and F. Foufelle. 2005. Anti-lipolytic action of AMP-activated protein kinase in rodent adipocytes. *J. Biol. Chem.* **280:** 25250–25257.
56. Tang, Y., and A. Chen. 2010. Curcumin prevents leptin raising glucose levels in hepatic stellate cells by blocking translocation of glucose transporter-4 and increasing glucokinase. *Br. J. Pharmacol.* **161:** 1137–1149.